

# Energy characteristics of tidal and residual level variations in the Okhotsk Sea from satellite altimetry data

Georgy Shevchenko<sup>1</sup> and Alexander Romanov<sup>2</sup>

<sup>1</sup> Institute of Marine Geology and Geophysics FEB RAS, Yuzhno-Sakhalinsk, Russia  
E-mail shevchenko@imgg.ru

<sup>2</sup> Federal State Unitary Enterprise Russian Institute of Satellite Device Engineering (FSUE "RISDE"), Moscow, Russia

## Abstract

A unified satellite altimetry database, TOPEX/Poseidon (1993–2002) and Jason-1 (2002–2007) containing about 7,000 locations, was created for the Okhotsk Sea and adjacent areas. Amplitudes and phases of main tidal constituents were calculated for each location, and maps of tidal character and height were constructed. It is shown that diurnal waves dominate in the amphidromic areas of semidiurnal waves in Sakhalinsky Bay, near the Yamskie Islands, and the eastern Sakhalin coastline. Tidal energy increases along the axis southwest–northeast and reaches maximal values in Shelikhov Bay. Root mean square amplitudes of residual time series were taken to represent non-tidal sea level variations. Areas with the highest values were considered to be energetic ocean zones. They have been found near the southeastern Kamchatka coast and on the Pacific shelf side of Hokkaido where mesoscale eddies are often observed. To a lesser extent they relate to the whole Kuril-Kamchatka deep trench (especially to its outside edge), as well as to the western Hokkaido shelf and northern Okhotsk Sea shelf where seasonal changes in currents are significant. A map showing the relative portion of tides and residual variations in total sea level energy has been constructed.

## Introduction

Satellite altimetry sea level data are used to study dynamic processes, such as tidal motions, seasonal sea level circulation changes and meso-scale eddy formations in different parts of World Ocean. Areas of high intensity sea level variations are interesting for many scientific and practical reasons. The Okhotsk Sea (OS) is one of these areas because of its very strong tides and non-tidal sea level variations. Satellite altimetry data give us very important information related to the dynamic processes in this area, especially in light of the small number of coastal tide gauges relative to the large area of the OS.

To determine areas with high intensity sea level variation (so-called energetic ocean zones) on the continental shelf and in the marginal seas is difficult because the Global Ocean Tide (GOT) model (Ray, 1999) is not exact enough to determine shallow water zones. To solve this problem, a special modification of the least squares method to determine tidal amplitudes and phases in each location of a sub-satellite track was developed (Shevchenko and

Romanov, 2004). This method is similar to the algorithm used by Cherniawsky *et al.* (2001). In this way, we estimated the average amplitude of tidal and residual (non-tidal) sea level variations as an index of energy zones in the OS and its adjacent areas.

## Data and Methods

TOPEX/Poseidon and Jason-1 satellite altimetry data were used as initial sea level data. These data were obtained from the NASA Physical Oceanography Distributed Active Archive Center at the Jet Propulsion Laboratory, California Institute of Technology.

For sea level calculation relative to a reference ellipsoid (the first-order definition of the non-spherical shape of the Earth as an ellipsoid of revolution with equatorial radius of 6378.1363 km and a flattening coefficient of 1/298.257) by satellite altimeter data, the following equation was applied:

$$H_y = H_c - (H_A + C_{WT} + C_{DT} + C_I + C_{EMB}) - H_{IB}, \quad (1)$$

where  $H_y$  is the sea level,  $H_c$  is the height of the

satellite's orbit,  $H_A$  is the altimetry range,  $C_{WT}$  is the wet troposphere correction,  $C_{DT}$  is the dry troposphere correction,  $C_I$  is the ionosphere correction,  $C_{EMB}$  is the electromagnetic bias correction, and  $H_{IB}$  is the inverse barometer correction.

All necessary corrections to the altimetry signal (except tidal GOT model corrections) were taken from a TOPEX/Poseidon MGDR-B dataset and were considered according to recommendations in Benada (2003). The standard technique described in Benada (2003) was used to obtain the reliability of altimetry data. A previously created (Shevchenko and Romanov, 2004, 2006) TOPEX/Poseidon sea level database (1993–2002) for the Okhotsk Sea and adjacent areas (northern Japan Sea, northwestern part of Pacific Ocean) was further developed using data of the Jason-1 satellite (2003–2007) which has the same orbits as TOPEX/Poseidon, and in a space 8 degrees southward. The total number of locations was about 7,000. The length of data sets varied significantly in different parts of the OS. Some gaps were due to ice cover, especially in the northwestern OS. For the area adjacent to Shantary Islands, the data sets were too short for the exact determination of tidal amplitudes and phases. Because of this problem, we did not analyse the sea level variations in this area.

Calculations of tidal amplitudes and phases were carried out for each location using the authors' method. The root mean square amplitude of the residual series ( $Ar$ ) was used to estimate the quality of the database. The exact attachment of Jason-1 data demanded additional mean sea level correction. Without this correction, the amplitude of the residual oscillations would have an unrealistically large value. By including the correction,  $Ar$  values were not more than 20 cm, and in the main part of the study area, not more than 10 cm. Usually residual variations on coastal tide gauges have a similar amplitude. We consider areas with high amplitude as energy production zones.

The average amplitude of 8 main tidal constituents (4 diurnal  $Q_1$ ,  $O_1$ ,  $P_1$ ,  $K_1$  and 4 semidiurnal  $N_2$ ,  $M_2$ ,  $S_2$ ,  $K_2$ ) is considered as an index of tidal variation intensity:

$$L = (H_{Q_1}^2 + H_{O_1}^2 + H_{P_1}^2 + H_{K_1}^2 + H_{N_2}^2 + H_{M_2}^2 + H_{S_2}^2 + H_{K_2}^2)^{1/2}. \quad (2)$$

Another index that is the relationship between amplitudes of main diurnal and semidiurnal waves is

$$R = (H_{O_1} + H_{K_1}) / (H_{M_2} + H_{S_2}), \quad (3)$$

which indicates zones where diurnal ( $R > 2$ ) and semidiurnal ( $R < 0.5$ ) waves predominate. Spatial distributions of  $L$ ,  $R$  and  $Ar$  were constructed for the OS and adjacent areas.

## Results and Discussion

The spatial distribution of the average tidal amplitude  $L$  is shown in Figure 1. This index increases from 25–30 cm in the southwestern part of the OS to 150 cm in the northeastern part. Maximal values (more than 200 cm) were found in Shelikhov Bay, in the northeastern part of the OS. In the 1980s, there was a plan to construct a tidal power station in this area (Bernstein, 1987). Some effects of the proposed station's dam on tidal amplitudes and phases were analysed by Nekrasov and Romanenkov (2003). They found that high tidal amplitudes occurred on the northern OS shelf, on the western shelf of Kamchatka peninsula, and in the northern part of Tatar Strait (Northern Japan Sea). Small amplitudes were detected in the central Japan Sea, in the southwestern OS and in the deep Pacific Ocean far from the Kuril Islands.

The spatial distribution of index  $R$  (Fig. 2) indicates a dominant role of diurnal tides in the OS that is in good agreement with the results of numerical simulations (Kowalik and Polyakov, 1998; Nekrasov and Romanenkov, 2003). We found areas with  $R$  values less than 1 near the northern OS coastline and in the part of the Pacific Ocean which is adjacent to Japan. As mentioned above, we did not analyse sea level variations in the area adjacent to the Shantary Islands where semidiurnal tides strongly predominate.  $R$  is high (greater than 2) in the middle part of the OS and on the northern and northeastern shelves of Sakhalin Island, especially in amphidromic areas in Sakhalinsky Bay and near the eastern Sakhalin coast. The same results were obtained for the semidiurnal tidal amphidrome near the Yamskie Islands. The presence of these amphidromes was first detected by Ogura (1933) as a result of coastal tide gauge data analysis, and is also verified by numerical modeling. An exception occurred for the east coast of Sakhalin, where an amphidrome was not identified by results of calculations at all (Kowalik and Polyakov, 1998). This amphidrome has an unusually large size due to its instability (Shevchenko and Romanov, 2004), and  $R$  reaches its highest values (greater than 10) here.

## Current dynamics

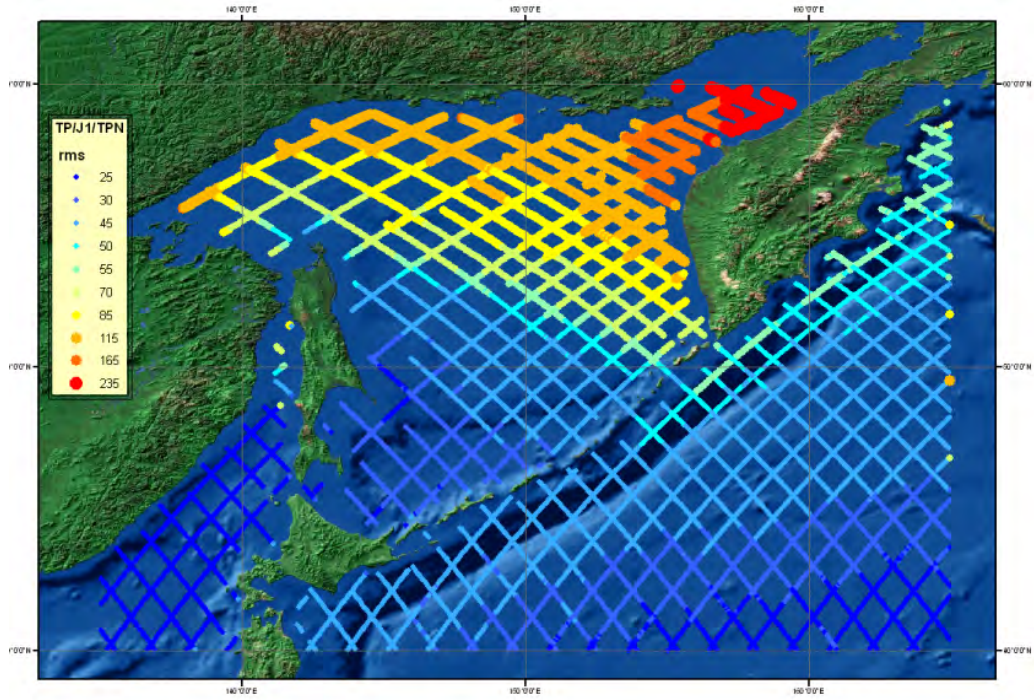


**Fig. 1** Spatial distribution of tidal root mean square amplitude  $L$  in the Okhotsk Sea and adjacent areas. TOPEX/Poseidon–Jason-1 sub-satellite tracks are shown.

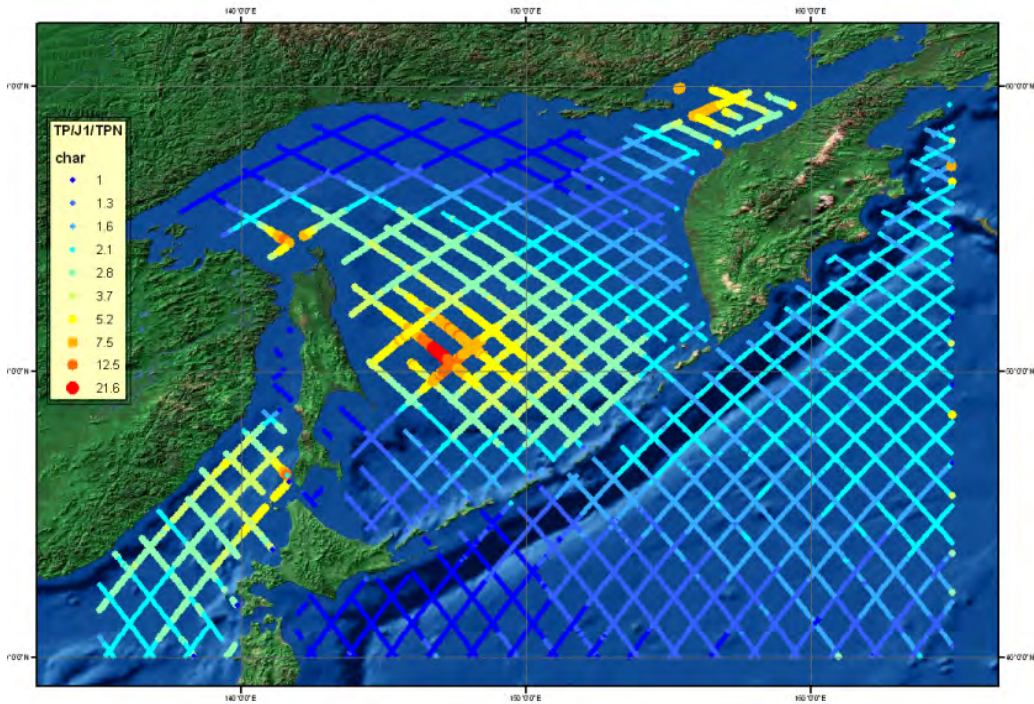


**Fig. 2** Spatial distribution of amplitudes of main diurnal and semidiurnal waves ( $R$ ).

The spatial distribution of the root mean square amplitude of residual sea level variations is shown in Figure 3. The Kuril–Kamchatka deep trench, especially in the areas adjacent to Hokkaido–South Kuril Islands and southeastern Kamchatka–North Kuril Islands, are energetic ocean zones. Both these areas are known as areas of intensive meso-scale eddy formation (Bulatov and Lobanov, 1983; Darnitsky and Bulatov, 2005). Another area with high  $Ar$  values is found in the deep trench (especially to its outside edge) near the middle part of the Kuril Ridge.

We found a zone of intensive eddy formation in the deep Kuril Basin in the southern part of the OS. High values of  $Ar$  are the result of strong seasonal sea level changes with a maximum in the wintertime and a significant negative surge in the fall (Romanov *et al.*, 2004). This negative surge is produced by strong and stable northerly and northwesterly winds which

are typical for autumn (so-called “winter monsoon”). The winter maximum corresponds to winter amplification of the Yamskoe and North Okhotsk Currents. Seasonal sea level changes in the area of the East Sakhalin Current are weaker in comparison to the northern OS shelf, so the eastern shelf of Sakhalin Island is not an area of high  $Ar$  values, in contrast to Sakhalinsky Bay and Amursky Liman. High seasonal sea level changes in these latter areas are induced by Amur River runoff. We also found some influence of Amur River runoff in the northern part of Tatar Strait, especially in the area adjacent to the mainland coastline. The area of the Tsushima Warm Current is also a region of high  $Ar$  amplitude. This effect is brought about by strong seasonal changes in the Current, which is weak in the wintertime and reaches maximal intensity in summer. In the central part of the OS, on the shelf of the Kuril Islands and in the area adjacent to western Kamchatka coast,  $Ar$  values are small, less than 10 cm.

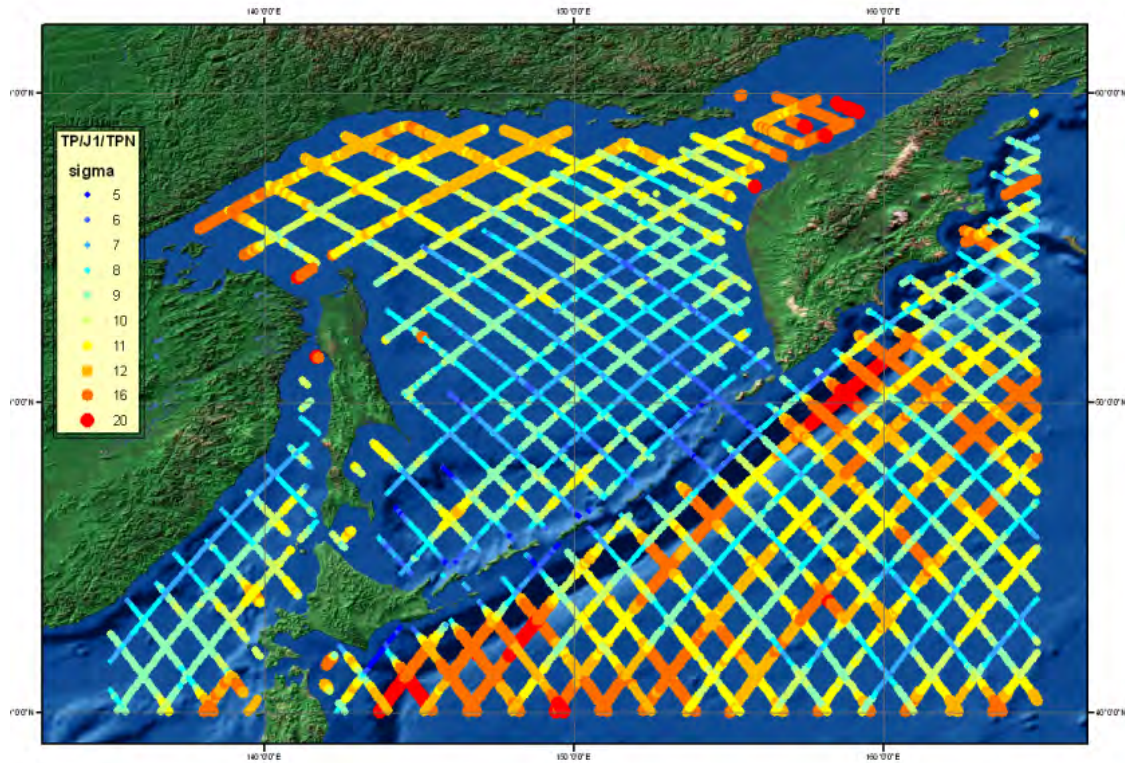


**Fig. 3** Spatial distribution of root mean square amplitude  $Ar$  residual level oscillations in the Okhotsk Sea and adjacent areas.

Figure 4 shows the spatial distribution of residual oscillation rates in total sea level variance (energy) in the study area. This rate is small (about 10–15%) in the northern, eastern, and especially the northwestern part of the OS because of very high tidal amplitudes. As stated above, the mean amplitude of residual oscillations is relatively high on the northern OS shelf. However, it is small in comparison with the tidal amplitude.

The influence of residual oscillations increases in southwestern part of the OS, especially in the deep

Kuril Basin, shallow Terpenia Bay and La Perouse Strait. In the Japan Sea, the rate of residual oscillations increases from the northern part of Tatar Strait to the western Hokkaido and northwestern Honshu shelves where it reaches 50–60% of total sea level variance. Similar values were found in the deep ocean area adjacent to Kuril Islands. The dominant role of residual oscillations is caused by both the decrease in tidal amplitude and the influence of Tsushima and Kuroshio currents seasonal changes and their meander formations.

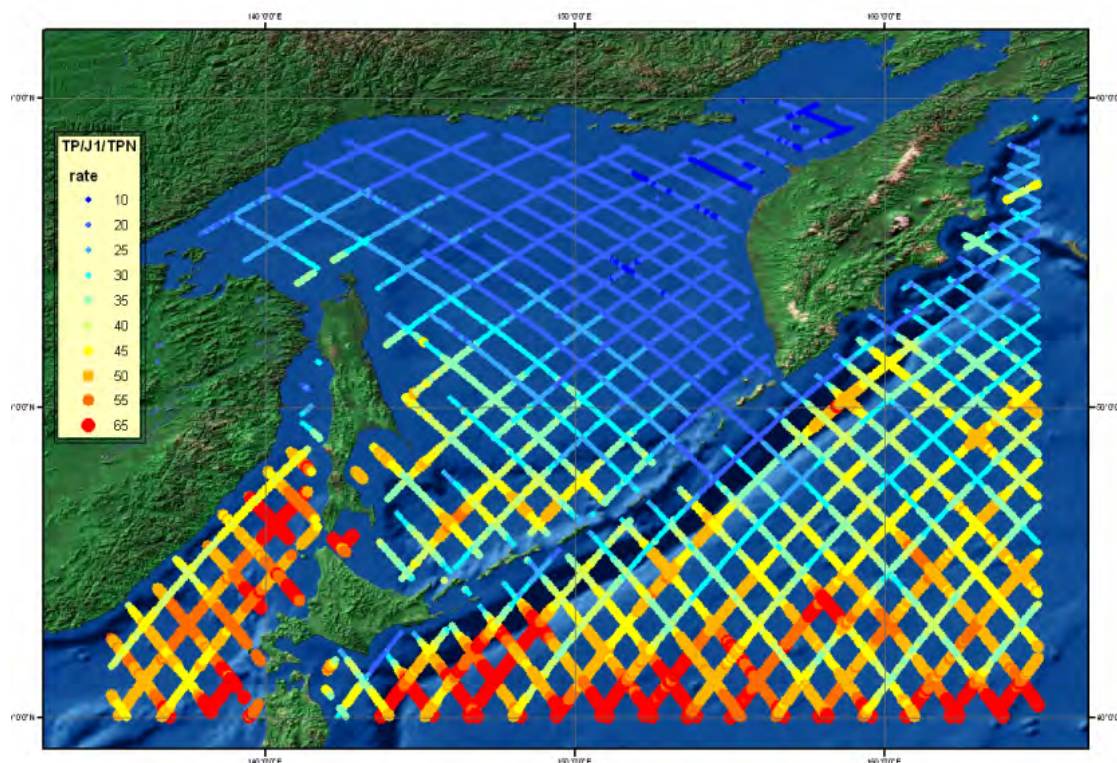


**Fig. 4** Spatial distribution of residual oscillation rates in total sea level variance in the OS and adjacent areas (%).

## Conclusions

Using a unified satellite altimetry database, TOPEX/Poseidon (1993–2002) and Jason-1 (2002–2007), spatial distributions of root mean square tidal and residual amplitudes were constructed for the OS and adjacent areas.

Diurnal tides were found to predominate over semidiurnal tides in the OS, with the exception of the northern shelf. The relation between amplitudes of main diurnal and semidiurnal tides  $R$  reaches

maximal values in the semidiurnal tide amphidromic areas (Yamskie Islands, Sakhalinsky Bay, eastern Sakhalin shelf). Tidal amplitude reaches maximal values in the northern, eastern, and especially northeastern parts of the OS. It is significantly smaller in the southwestern part of OS, in the central part of Japan Sea, and in the Pacific Ocean far from the Kuril Ridge.

The mean amplitude of residual oscillations indicates zones of intensive eddy formations in the deep Kuril–Kamchatka Trench. Its maximal values are

found in the areas adjacent to Hokkaido–South Kuril Islands and southeastern Kamchatka–North Kuril Islands; smaller values are found in the area of the Middle Kuril Islands. High residual amplitudes on northern OS shelf and western Hokkaido shelf are caused by seasonal changes of sea level and circulation.

### Acknowledgement

This work was sponsored by the Russian Foundation of Basic Research (grant 07-05-00637-a).

### References

- Bernstein, L.B. 1987. Tidal Power Stations. Energoatomizdat, Moscow, 296 pp. (in Russian).
- Benada, J.R. 2003. Merged GDR (TOPEX/POSEIDON) Generation B Handbook Version 2.
- Bulatov, N.V. and Lobanov, V.B. 1983. Investigation meso-scale eddies easterly of Kuril Islands from meteorological Earth's satellite data. *J. Earth Res. Space* **3**: 40–47 (in Russian).
- Cherniawsky, J.Y., Foreman, M.G.G., Crawford, W.R. and Henry, R.F. 2001. Ocean tides from the TOPEX/POSEIDON sea level data. *J. Atmos. Oceanic Technol.* **18**: 649–664.
- Darnitsky, V.B. and Bulatov, N.V. 2005. Structure elements and meso-scale eddy evolution underwater mountains Erimo – Takuie: remote and in-situ observations. *Comm. Fish. Oceanogr.* **2**: 277–302 (in Russian).
- Kowalik, Z. and Polyakov, I. 1998. Tides in the Sea of Okhotsk. *J. Phys. Oceanogr.* **28**: 1389–1409.
- Nekrasov, A.V. and Romanenkov, D.A. 2003. Prognostic estimation of tidal sea level transformation as result of lager-scale construction in the Beloe and Okhotsk Seas. Level oscillations in seas. Russian State Hydrometeorological University, St. Peterburg, pp. 57–78 (in Russian).
- Ogura, S. 1933. The tides in the seas adjacent to Japan. Bull. Hydrographic Dept., Imp. Japan Navy, Vol.7, Tokyo.
- Ray, R.D. 1999. A global ocean tide model from Topex/Poseidon altimetry: GOT99.2. – NASA Tech. Memo. 209478.
- Romanov, A.A., Sedaeva, O.S. and Shevchenko, G.V. 2004. Seasonal level changes in the Okhotsk Sea from coastal tide gauges and satellite altimetry data. *J. Earth Res. Space* **6**: 59–72 (in Russian).
- Shevchenko, G.V. and Romanov, A.A. 2004. Tides characteristics in the Sea of Okhotsk definition from Topex/Poseidon sea level data. *J. Earth Res. Space* **1**: 49–62 (in Russian).
- Shevchenko, G.V. and Romanov, A.A. 2006. Seasonal changes of circulation in the upper layer of the Sea of Okhotsk from satellite altimetry data. *Russian Meteorol. Hydrol.* **8**: 59–71 (in Russian with English translation).